Atmospheric
Chemistry
and Physics

Supplement of

Aqueous-phase reactive species formed by fine particulate matter from remote forests and polluted urban air

Haijie Tong et al.

Correspondence to: Haijie Tong (h.tong@mpic.de, haijie.tong@polyu.edu.hk)

Influence of PM$_{2.5}$ extract concentration on the radical yield.

To assess the influence of the PM$_{2.5}$ extract concentrations on our results, we compared the mass-specific radical yields by different concentration of Beijing PM$_{2.5}$ extracts. We found the yield difference is on average for 37% among all extract samples. However, we did not see clear trend from low to high concentration of PM$_{2.5}$ extracts. Then we showed the PM$_{2.5}$ extract concentrations of each sample as well as the radical yields by different concentration of PM$_{2.5}$ extracts in Figure S1. Figures S1a-1c indicate that PM$_{2.5}$ extract concentrations of Hyytiälä and Mainz samples have narrower range distribution than Beijing samples. Figure S1d and 1e showed that radical yields by 500 µg mL^{-1} fine PM$_{2.5}$ overlapped the yields by 250-6400 µg mL^{-1} PM. Thus, the concentration of the PM$_{2.5}$ extracts has small impact on our results about RS yields. To evaluate the influence of PM$_{2.5}$ extract concentrations on the relative yields of different radicals, we measured the relative yields of different radicals by Beijing PM$_{2.5}$ (n=3) in 250, 500, and 1000 µg mL^{-1} PM$_{2.5}$ extracts. We found the relative yields of $^\bullet$OH, O$_2^{\bullet-}$, C- and O-centered organic radicals have standard deviations of ~10%, ~9%, ~2%, and ~2%, respectively.

Estimation of the abundance of organic hydroperoxides and humic-like substances in PM$_{2.5}$

Based on the compiled abundance of humic-like substances in PM$_{2.5}$ (Table S3), we obtained an averaged value of 7%, and we assumed that 15% of these PM$_{2.5}$-bound humic-like substances are extractable humic acid-like substances (Katsumi et al., 2019). Given that the concentration of PM$_{2.5}$ in aqueous extracts in this study ranged from 250 to 6500 µg mL^{-1}, thus the estimated concentration of humic acid-like substances typically ranged from 3 to 70 µg mL^{-1}. We assumed that 75% of the PM$_{2.5}$-bound humic-like substances are attributable to humic acid-like substances, thus the estimated concentration of extractable fulvic acid-like substances typically ranged from 15 to 350 µg mL^{-1}. To simulate the RS formation by Mainz and Beijing PM$_{2.5}$, we used 4 µg mL^{-1} humic acid standard. To investigate the influence of humic-like substances on the RS formation by Fenton-like reactions, we used 6-180 µg mL^{-1} humic or fulvic acid for surrogate mixture measurements. HA or FA are used in this study as standard surrogate compounds for humic-like substances and are known to only partly dissolve in water (Baduel et al., 2009;Verma et al., 2015). Thus, it is difficult to generate an equivalent concentration of a HA or FA suspension that can

represent the water-soluble and insoluble fractions of humic-like substances contained in one ambient $PM_{2.5}$ sample. Only by keeping the initial concentration of aqueous-phase HA or FA known, the chemical reaction mechanism of the surrogate compounds can be understood quantitatively. Beyond this, the co-existence of solid phase and aqueous-phase HA or FA in the surrogate solutions will complicate the chemistry of the surrogate compounds upon potentially inducing surface adsorption and surface chemistry effects. Thus, for simplicity, we only analyzed the water-soluble fraction of HA or FA in this study.

To estimate the abundance of organic hydroperoxide in ambient $PM_{2.5}$, we assumed that the mass fractions of SOA in Hyytiälä, Mainz, and Beijing $PM_{2.5}$ were 60%, 25%, and 15%, respectively (Jimenez et al., 2009). We also assumed that 2%, 2%, and 1% of Hyytiälä, Mainz, and Beijing SOA mass are attributable to organic hydroperoxides (Tong et al., 2018), which was assumed to have an averaged molecular weight of 300 g moL^{-1} (Docherty et al., 2005). In this case, the estimated concentration of organic hydroperoxides in the $PM_{2.5}$ extracts in this study was 5-35 µM. To simulate the RS formation by Hyytiälä, Mainz, and Beijing fine $PM_{2.5}$, we used 50, 25, and 0 µM cumene hydroperoxide (CHP), respectively. To investigate the RS yield of Fenton-like reactions, we used 50-100 µM CHP.

To note, there is a gap between the concentration of gas phase O_3 or •OH in laboratory chamber experiment and ambient air. In the PAM chamber, one might form atmospherically irrelevant RS under the high oxidant conditions (Peng and Jimenez, 2020). The distributions and identities of HOM in SOA depend on the absolute concentrations of O_3 or •OH and also the concentration ratio of oxidant to precursor, which warrants further analysis.

Due to the technique limitation, we are not able to quantify different aromatic or HOM species. In contrast, the method for quantification of water-soluble transition metals is well-established. Therefore, we can obtain reliable results on the absolute concentrations of target transition metals in Hyytiälä, Mainz, and Beijing PM or their water extracts.

Selection of SOA precursors

Monoterpenes have been found as major volatile organic compounds (VOC) in Hyytiälä, and α- and β-pinene are isomers accounting for > 60% of the total VO C (Kourtchev et al., 2008;Hakola et al., 2012).

Previous studies found that both α- and β-pinene exhibit high SOA yield upon oxidation by O_3 (Lee et al., 2006;Zhang et al., 2015), and β-pinene SOA exhibits a higher potential in generating RS in water (Tong et al., 2016;Tong et al., 2017;Tong et al., 2018;Tong et al., 2019). To shorten the collection time of SOA and minimize the influence of aerosol aging on the aqueous RS detection, β-pinene was chosen as representative biogenic precursor for the SOA formation in Hyytiälä. In contrast, naphthalene has been found as key anthropogenic VOC in Beijing, which has high SOA yield upon photooxiation and potentially important contribution to SOA formation in Beijing (Chan et al., 2009;Huang et al., 2019). Recently studies also indicate that naphthalene SOA are redox-active substances and may play an important role in cytotoxicity of Beijing PM (Liu et al., 2020;Han et al., 2020). Thus, we choose naphthalene as representative anthropogenic precursor for the SOA formation in Beijing.

The mass-specific radical yield of laboratory-generated SOA is strongly dependent on the abundance of peroxide-containing highly oxygenated organic molecules (Tong et al., 2019), which may involve in the radical formation upon thermal-, hydrolytic-, and photolytic- decompositions as well as Fenton-like reactions in water (Chen et al., 2011;Badali et al., 2015;Tong et al., 2016). Previous studies found that the mass fraction of organic peroxides in β-pinene SOA (42%) can be two times higher than in Naphthalene SOA (19-28%) (Kautzman et al., 2010;Tong et al., 2018). Our recent findings also confirmed the positive correlation of HOM abundance and radical yields by both ambient PM and laboratory-generated SOA (Tong et al., 2019). Therefore, we suggest that the low abundance of peroxide-containing HOMs in naphthalene SOA is the major reason for its lower radical yield than β-pinene SOA.

H_2O_2 yield of PM from other sources

The air sample volume-specific and mass-specific H_2O_2 yields as well as total RS yields of fine PM from other sites that different from Hyytiälä, Mainz, and Beijing are shown in Figure S4 and Table S5. Therein the H_2O_2 yields were measured using *p*-hydroxyphenylacetic acid (PHOPAA) as probe, and the total RS yields were measured using dichlorofluorescin (DCFH) assay as probe (Lazrus et al., 1985;Wang and Joseph, 1999;Kalyanaraman et al., 2012). Figure S4a shows that the air sample volume-specific H_2O_2 yields of fine PM from CRC-AES and different districts of UCLA exhibit a positive correlation with the

concentration of $PM_{2.5}$ ($R^2=0.60$). In contrast, the mass-specific H_2O_2 yields exhibit no correlation with the $PM_{2.5}$ concentration ($R^2=0.02$, Figure S4b). Moreover, the DCFH-based total RS yields were overall higher than the H_2O_2 (Table S5), agreeing with this study.

Influence of HA and FA on the radical yields of Fenton-like reactions initiated by Cu^{2+}

Figure S6a shows that the concentration of radicals formed by Cu^{2+} and cumene hydroperoxide (CHP) mixtures exhibited a positive correlation with the concentration of Cu^{2+}. However, the Cu^{2+} played a less effective role than Fe^{2+} in initiating Fenton-like reactions via radical formation pathways, with 300 µM Cu^{2+} and 50 µM CHP produced ~1.8 µM radicals.

Figure S6b shows that as the concentration of Cu^{2+} increased from 15 to 75 µM, the RF of $^\bullet OH$ and $O_2^{\bullet-}$ decreased from ~44% to ~18% and from ~1.6% to ~0.1%. However, the RF of C- and O-centered organic radicals increased from~39% to ~61% and from ~15% to ~21%, respectively. As the concentration of Cu^{2+} is increased further to 150 and 300 µM, the RF of $^\bullet OH$, $O_2^{\bullet-}$, C- and O-centered organic radicals varied slightly, reflecting a low reactivity of Cu^{2+} with CHP.

Figure S6c shows that concentration of radicals formed by reactions of 100 µM CHP with 300 µM Cu^{2+} and HA decreased from ~2.3 to ~1.8 µM as the increasing of HA concentration from 0 to 180 µg mL^{-1}. Beyond this, humic-like substances have been found to exhibit strong copper-binding ability (Kogut and Voelker, 2001), and 8-fold more Cu^{2+} than Fe^{2+} ions from Melpitz (Germany) PM were expected to be complexed by humic-like substances (Scheinhardt et al., 2013). We thus inferred that the Cu-HA complex might significantly influence the reactivity of Cu^{2+} in Fenton-like reactions. Finally, partial of the radical yield decay in Figure S6a might be caused by the antioxidant effect of HA (Aeschbacher et al., 2012). Figure S6d shows that as the concentration of HA increased from 6 to 180 µg mL^{-1}, the RF of $^\bullet OH$ and O-centered organic radicals increased from ~17 to ~44% and from ~16 to ~28%, respectively. The RF variation of $^\bullet OH$, C- and O-centered organic radicals in Figure S6d had a different trend from the results in Figure 6f, reflecting different impacts of HA on Cu and Fe initiated Fenton-like reactions. Compared to the

increasing RF of $^{\bullet}$OH and O-centered organic radicals, the RF of C-centered radicals decreased from ~66 to ~28%, and the RF of $O_2^{\bullet-}$ only varied slightly between 0.8 and 1.5%.

Figure S6e shows that the radical yields of the mixtures consisting of 100 µM CHP, 300 µM Cu^{2+}, and FA only varied from ~0.9 to ~0.4 µM as the increasing FA concentration from 6 to 180 µg mL^{-1}, which may mainly be associated with the low catalytic effect of Cu^{2+} as well as the formation of Cu-FA complexes. Figure S6f indicates that as the concentration of FA increased from 0 to 180 µg mL^{-1}, the RF of C-centered radicals steeply increased from ~57 to ~89%, whereas the RF of O-centered organic radicals and $^{\bullet}$OH exhibited overall decrease from ~25% and ~16% to ~3%.

To note, there are multiple sinks of the BMPO-radical adducts, which include the conversion of BMPO-OOH to BMPO-OH, direct dissociation, and reactions with other reactants (e.g., metal ions and radicals) in the aqueous extracts of PM (Tong et al., 2018). It remains a challenge to assess the influence of decomposition products of BMPO-radical adducts on the radical detection in this study, warranting further studies.

Influence of O_2 on the radical formation of SOA

Aqueous-phase O_2 has been suggested to be capable of inducing autooxidation reactions and influencing the Fenton-like chemistry as well as HO_x cycles of organic hydroperoxides in water (Floyd and Wiseman, 1979;Chevallier et al., 2004). We thus compared the radical yields of β-pinene SOA in non-degassed and degassed water (with ultrapure N_2 for ~1 h and keep the N_2 exposure during the extraction operation). We found that OH radicals are always the major species trapped by BMPO and detected with EPR within both environments. Moreover, ~20% more radicals were observed upon dissolving β-pinene SOA in non-degassed water (1 mM), reflecting the important role of O_2 in the radical formation by SOA in water. These experimental results can be explained by our recent modelling analysis, which shows that absence of O_2 will lead to the recombination of C-centered radicals $R^{\bullet}$ and interrupt formation of peroxy radicals and superoxide radicals from $R^{\bullet}$ (Tong et al., 2017;Tong et al., 2018). In this study, measurements were

conducted under ambient, non-degassed conditions. We assume that the concentration of oxygen in the aqueous phase (~0.29 mM) is determined by Henry's law and remain constant over reaction time.

Table S1. **Sampling information and mass concentrations of fine particulate matter (PM$_{2.5}$).**

City	Location	PM size	PM$_{2.5}$ concentration ($\mu g\ m^{-3}$)	Flow rate (L min^{-1})	Sampling time (h) [a]	Sampling period	Sample numbers
Hyytiälä	61.51°N, 24.17°E	≤ 2.5 μm	4.6±1.1	30	48-72	31 May-19 July 2017	11
Mainz	49.99°N, 8.23°E	0.056-1.8 μm	15.5±0.8	30	24-54	22 Aug.-17 Nov. 2017 23-31 Aug. 2018	11
Beijing	116.31°E, 39.99°N	≤ 2.5 μm	201.5±46.3	30	5-24	20 Dec. 2016-13 Jan. 2017 6 Nov. 2017-17 Jan. 2018	20

[a] The sampling time is for one filter

[b] MOUDI: Micro-Orifice Uniform Deposition Impactor (122R)

Table S2. The range of hyperfine coupling constants that used to fit the BMPO adducts.

Spin adduct	Hyperfine coupling constant (G)		
	a_N	a_H^β	a_H^γ
BMPO-OH1	12-16	11-12	0.5-0.9
BMPO-OH2	14-15	13-14	0.6-0.7
BMPO-OOH1	13-14	8-10	—
BMPO-OOH2	13-14	11-13	—
BMPO-C-centered radicals	14-16	21-23	—
BMPO-O-centered organic radicals	14-16	17-18	—

Table S3. **Abundance of humic-like substances in ambient PM$_{2.5}$.**

Location	Time/event	PM$_{2.5}$ (µg m^{-3})	humic-like substances (µg m^{-3})	humic-like substances /PM$_{2.5}$ (%)	Reference
Lanzhou	Winter	120.47	7.24	6.0	(Tan et al., 2016)
Lanzhou	Summer	34.12	2.15	6.3	(Tan et al., 2016)
Lanzhou	Annual	77.29	4.7	6.1	(Tan et al., 2016)
Lanzhou	Haze	182.08	10.06	5.5	(Tan et al., 2016)
Lanzhou	No-haze	51.65	3.49	6.8	(Tan et al., 2016)
Lanzhou	Snow	80.69	4.62	5.7	(Tan et al., 2016)
PRD[a]	Annual 2007-2008	49	4.9	10.0	(Lin et al., 2010)
Guangzhou	Annual 2009	56	4.8	8.6	(Kuang et al., 2015)
Beijing	Winter 2011	108	8.9	8.2	(Lang et al., 2017)
Beijing	Summer	98	5.5	5.9	(Li et al., 2019)
Beijing	Autumn	58	5.6	9.4	(Li et al., 2019)
Beijing	Winter	150	12.3	7.9	(Li et al., 2019)
Beijing	Spring	120	6.5	4.8	(Li et al., 2019)
Average		91.2	6.2	7.0	

PRD: Pearl River Delta Region in China

Table S4. Measurement results for investigated aerosol samples: air sample volume- and mass-specific concentrations of aqueous-phase radicals and water-soluble metal ions in water.

Location	H_2O_2 (pmol m^{-3})	Radicals (pmol m^{-3})				Water-soluble transition metals (pmol m^{-3})				
		$^{\bullet}OH$	C-centered	O-centered organic	$O_2^{\bullet-}$	Fe	Mn	Cu	V	Ni
Hyytiälä	10.2 ± 7.9	0.4 ± 0.2	2.2 ± 1.4	0.1 ± 0.1	0.02 ± 0.01	26.0 ± 16.0	4.9 ± 4.8	3.1 ± 1.2	2.5 ±1.7	0.04± 0.01
Mainz	46.6 ± 16.6	2.1 ± 1.3	1.8 ± 0.7	0.2 ± 2	0.1 ± 0.1	269.0 ± 113.0	28.0 ± 12.0	55.0 ± 17.0	2.9 ± 0.8	1.2 ± 0.4
Beijing	195.9 ± 118.1	3.6 ± 2.6	2.5 ± 1.7	0.3 ± 0.2	0.2 ± 0.3	3300.0 ± 2300.0	640.0 ± 531.0	452.0 ± 385.0	23.0 ± 23.0	51.0 ± 25.0

| Location	H_2O_2 (pmol µg^{-1})	Radicals (pmol µg^{-1})				Water-soluble transition metals (pmol µg^{-1})				
		$^{\bullet}OH$	C-centered	O-centered organic	$O_2^{\bullet-}$	Fe	Mn	Cu	V	Ni
Hyytiälä	1.9 ± 0.9	0.08 ± 0.004	0.5 ± 0.2	0.03 ± 0.01	0.01 ± 0.01	5.5 ± 1.5	1.0 ± 0.5	0.7 ± 0.3	0.5 ± 0.2	0.01 ± 0.003
Mainz	3.3 ± 1.1	0.2 ± 0.1	0.1 ± 0.07	0.02 ± 0.02	0.01 ± 0.01	18.0 ± 4.9	1.9 ± 0.7	3.9 ± 0.6	0.2 ± 0.03	0.08 ± 0.03
Beijing	3.4 ± 5.6	0.04 ± 0.04	0.02 ± 0.02	0.003 ± 0.002	0.002 ± 0.002	20.0 ± 7.0	4.5 ± 2.6	2.3 ± 0.4	0.2 ± 0.2	0.5 ± 0.5

Table S5. Statistic of H_2O_2 or RS yields of ambient PM in water at different locations.

Sampling site	PM type	PM ($\mu g\ m^{-3}$)	Sampling time	Method	Analyte	H_2O_2 or RS (pmol m^{-3})	H_2O_2 or RS (pmol μg^{-1})	Reference
Hyytiälä	$PM_{2.5}$	5 ± 2	Jun-Jul 2017	MAK165	H_2O_2	10.2 ± 7.9	1.9 ± 0.9	This study
UCLA Pacific coast	Fine	13 ± 10	May 2014-Jan 2015	PHOPAA+HRP	H_2O_2	12 ± 9	1.0 ± 0.9	(Arellanes et al., 2006)
MPI-C at Mainz	$PM_{1.8}$	16 ± 2	Aug-Sep 2017	MAK165	H_2O_2	46.6 ± 16.6	3.3 ± 1.1	This study
UCLA	$PM_{2.5}$	16 ± 7	2009-2010	PHOPAA+HRP	H_2O_2	47 ± 21	3.0 ± 2.0	(Wang et al., 2012)
CRC-AES, UC Riverside	$PM_{2.5}$	19 ± 6	Jun-Aug 2008	PHOPAA+HRP	H_2O_2	$(2.7 \pm 2.1) \times 10^2$	1.4 ± 1.6	(Wang et al., 2012)
UCLA freeway site	Fine	23 ± 8	Jan-May 2004	PHOPAA+HRP	H_2O_2	17 ± 90	0.7 ± 1.1	(Arellanes et al., 2006)
UCLA Pacific coast	Coarse	26 ± 15	Jul 2004	PHOPAA+HRP	H_2O_2	31 ± 9	1.2 ± 0.6	(Arellanes et al., 2006)
UCLA freeway site	Coarse	27 ± 33	Jul 2004	PHOPAA+HRP	H_2O_2	15 ± 9	0.6 ± 0.3	(Arellanes et al., 2006)
UC Riverside campus	$PM_{2.5}$	39 ± 22	Aug 2005	PHOPAA+HRP	H_2O_2	$(1.2 \pm 1.1) \times 10^3$	28.0 ± 20.0	(Wang et al., 2012)
UCLA campus	Coarse	46 ± 22	Aug 2005	PHOPAA+HRP	H_2O_2	$(5.0 \pm 2.4) \times 10^2$	14.1 ± 9.4	(Wang et al., 2010)
UCLA upwind Riverside	Coarse	97 ± 27	Jun-Aug 2008	PHOPAA+HRP	H_2O_2	$(1.0 \pm 0.4) \times 10^3$	10.9 ± 5.3	(Wang et al., 2010)
Beijing	$PM_{2.5}$	201 ± 160	Dec 2016- Jan 2017	MAK165	H_2O_2	195.9 ± 118.1	3.4 ± 5.6	This study
Taipei	Coarse	7.5 ± 2.8	Jul-Sep 2000	DCFH+HRP	RS	64 ± 33	8.5 ± 11.8	(Hung and Wang, 2001)
Bern	$PM_{2.5}$	10 ± 5	Nov 2014	DCFH+HRP	RS	$(4.9 \pm 2.9) \times 10^2$	50	(Zhou et al., 2018)

Location	PM type	Concentration	Date	Method				Reference
Atlanta	PM$_{2.5}$	10.5 ± 3.2	12-17 Jul 2012	DCFH+HRP	RS	$(1.6 \pm 0.2) \times 10^2$	14.8 ± 4.5	(King and Weber, 2013)
Atlanta	PM$_{2.5}$	11.5 ± 4.3	8-31 May 2012	DCFH+HRP	RS	$(2.6 \pm 0.1) \times 10^2$	22.6 ± 3.0	(King and Weber, 2013)
Atlanta	PM$_{2.5}$	13.2 ± 4.8	8-29 Jun 2012	DCFH+HRP	RS	$(1.4 \pm 0.1) \times 10^2$	10.6 ± 1.9	(King and Weber, 2013)
Atlanta	PM$_{2.5}$	13.2 ± 5.4	3-31 Jul 2012	DCFH+HRP	RS	$(2.4 \pm 0.1) \times 10^2$	18.2 ± 1.8	(King and Weber, 2013)
London	PM$_{2.5}$	5-28	not reported	DCFH+HRP	RS	$(0.4\text{-}2.4) \times 10^4$	not reported	(Wragg et al., 2016)
Singapore (campus)	PM$_{2.5}$	19 ± 2	Dec 2005	DCFH+HRP	RS	$(5.7 \pm 0.7) \times 10^3$	0.3	(See et al., 2007)
Taipei	PM$_{3.2}$	31 ± 15	Jul-Sep 2000	DCFH+HRP	RS	$(5.4 \pm 0.5) \times 10^2$	17.6 ± 29.2	(Hung and Wang, 2001)
Singapore (curbside)	PM$_{2.5}$	33 ± 6	Dec 2005	DCFH+HRP	RS	$(1.5 \pm 0.2) \times 10^4$	460	(See et al., 2007)
Milan (traffic site)	TSP	50 ± 7	July 2013	DCFH+HRP	RS	$(1.4 \pm 0.7) \times 10^2$	2.73 ± 1.29	(Perrone et al., 2016)
Milan (low emission zone)	TSP	52 ± 19	Oct 2013	DCFH+HRP	RS	$(2.0 \pm 1.1) \times 10^2$	3.74 ± 1.41	(Perrone et al., 2016)
Milan (traffic site)	TSP	57 ± 19	Oct 2013	DCFH+HRP	RS	$(2.4 \pm 1.3) \times 10^2$	4.02 ± 1.77	(Perrone et al., 2016)
Beijing	PM$_{2.5}$	5-110	Aug-Sep 2015	DCFH+HRP	RS	$(0.2\text{-}3.6) \times 10^4$	not reported	(Huang et al., 2018)
Beijing	PM$_{2.5}$	74 ± 58	Dec 2014	DCFH+HRP	RS	$(1.3 \pm 0.5) \times 10^4$	179.6 ± 87.8	(Huang et al., 2016)
Beijing	PM$_{2.5}$	79 ± 59	Apr 2015	DCFH+HRP	RS	$(5.8 \pm 2.6) \times 10^3$	73.6 ± 43.4	(Huang et al., 2016)
Milan (traffic site)	TSP	129± 60	Jan-Feb 2013	DCFH+HRP	RS	$(3.6 \pm 0.8) \times 10^2$	2..99 ± 1.52	(Perrone et al., 2016)
Rubidoux, CA	PM$_{2.5}$	not reported	Jul 2003	DCFH+HRP	RS	$(4.7 \pm 0.4) \times 10^3$	not reported	(Venkatachari et al., 2005)
Rochester, NY	PM$_{2.5}$	not reported	Aug 2009	DCFH+HRP	RS	$(8.3 \pm 2.2) \times 10^3$	not reported	(Wang et al., 2011)

2
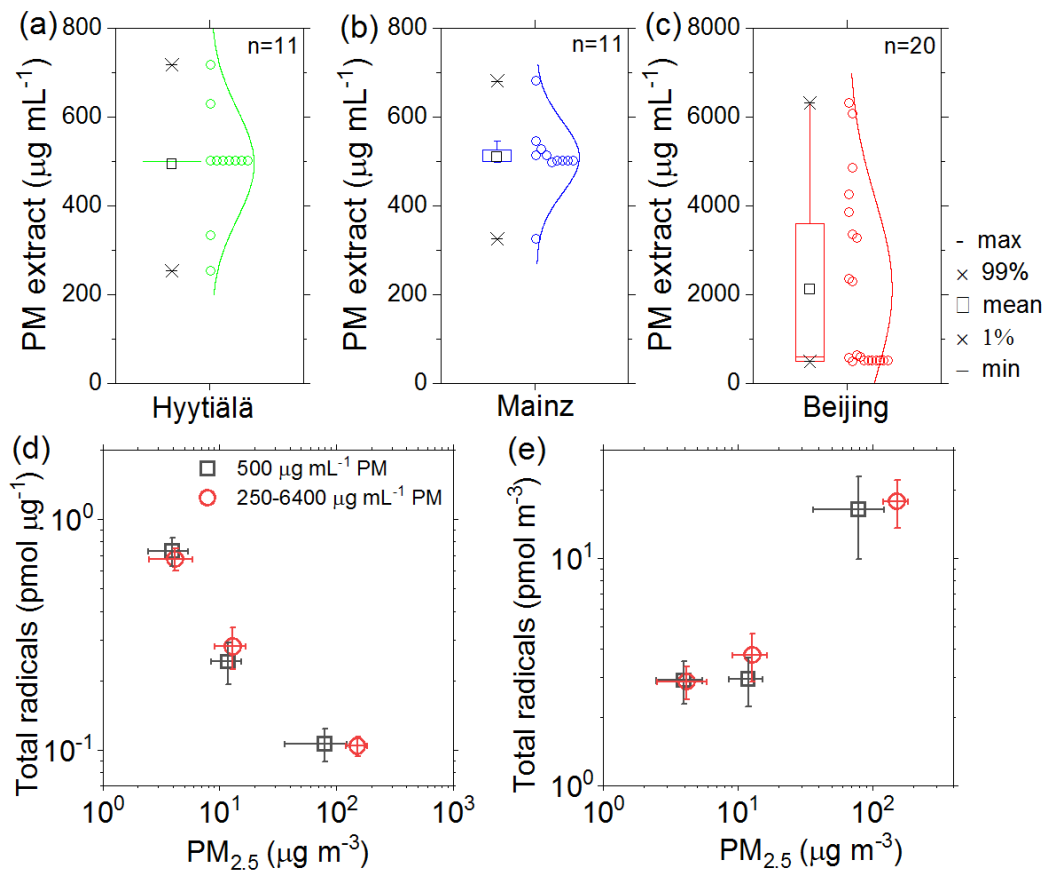
Figure S1. (a-c) Concentrations of $PM_{2.5}$ in aqueous extracts of each filter samples. (d) Mass-specific radical yields by different concentrations of $PM_{2.5}$ in water versus the concentration of ambient $PM_{2.5}$ in air. (e) Air sample volume-specific radical yields by different concentrations of PM versus the concentration of ambient $PM_{2.5}$. The error bars denote the standard errors (11-20 samples per location).
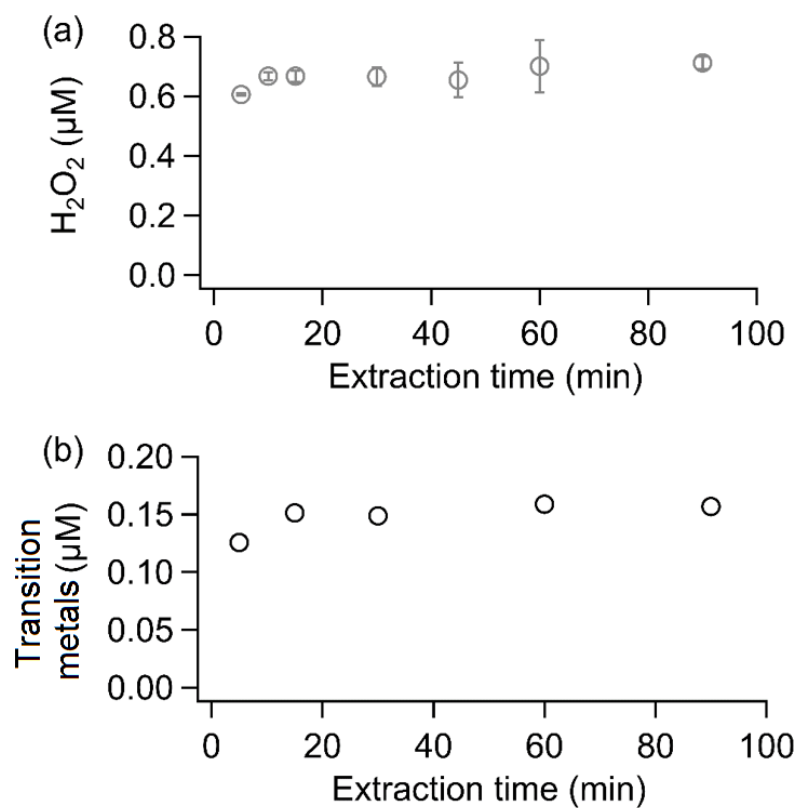
Figure S2. (a) Temporal evolution of H_2O_2 concentration in water extracts during the extraction process. Error bars represent standard deviation of duplicate measurements. (b) Temporal evolution of water-soluble transition metal concentration in water extracts during the extraction process. The H_2O_2 and transition metal concentrations became constant after ~15 min's extraction. The filter used for these tests was collected at Mainz from 25 to 27 Oct. 2017.
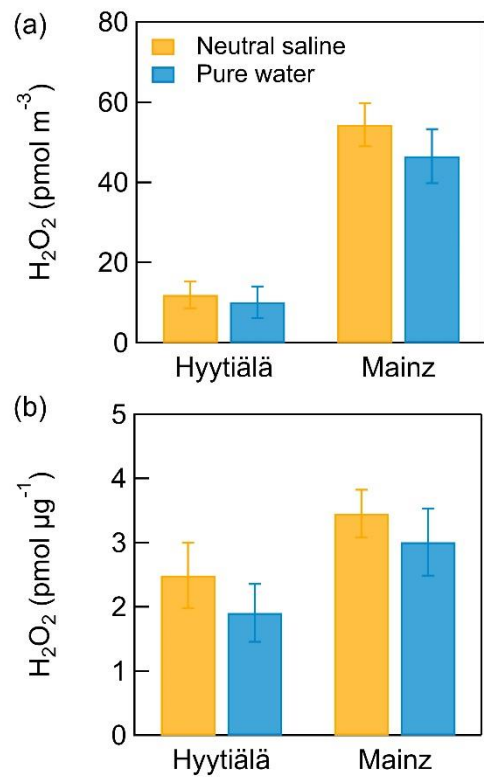
Figure S3. (a) Air sample volume-specific and (b) mass-specific H_2O_2 yield of Hyytiälä and Mainz fine PM in neutral saline (yellow column) and pure water (blue column). The error bars represent standard deviations of mean (11-12 samples per location).
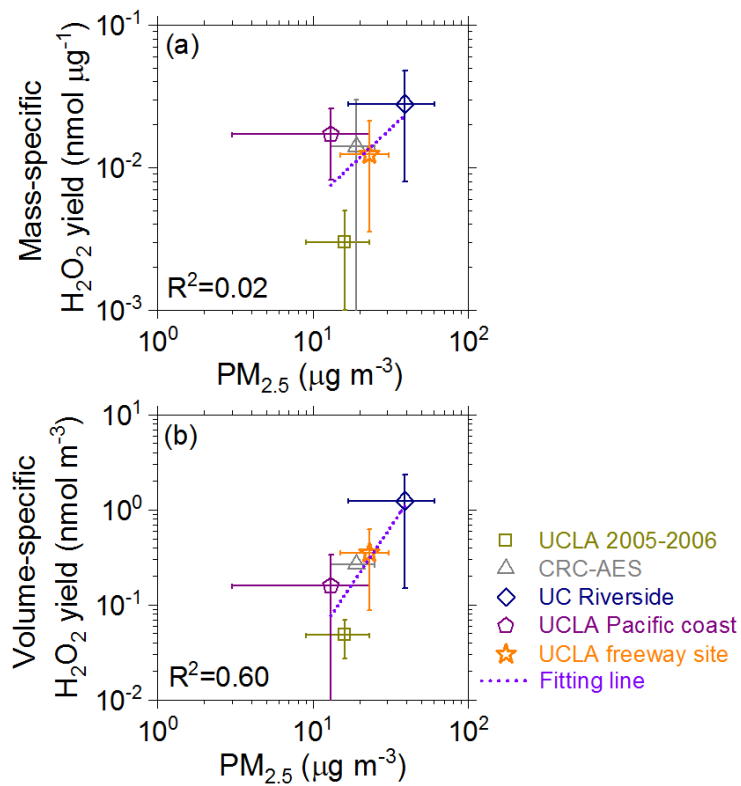
Figure S4. (a) Mass-specific and (b) air sample volume-specific H_2O_2 and RS yields of PM from different sites. The error bars represent standard deviation.
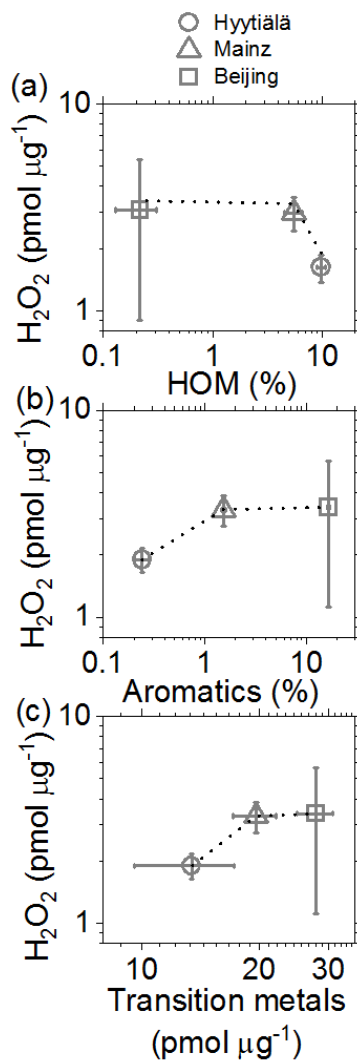
Figure S5. Correlation of (a) highly oxygenated organic molecules (HOM), (b) aromatics, and (c) water-soluble transition metals in ambient $PM_{2.5}$ with mass-specific yields of observed aqueous-phase H_2O_2. The error bars represent standard errors of the mean (4 to 12 samples per location). The dashed lines are to guide the eye.
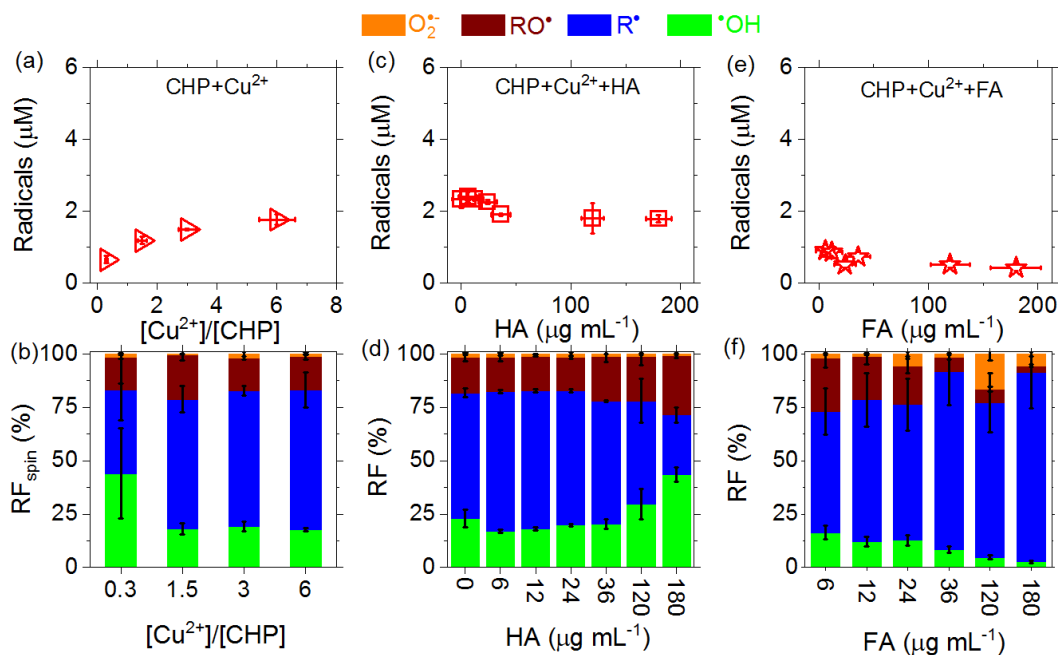
Figure S6. (a, c, e) Concentration of totally formed radicals (spins) and (b, d, f) RF_{spin} of individual radicals in aqueous mixtures comprising CHP, Cu^{2+}, HA, or FA. The concentration of CHP in (a) and (b) is 50 µM. The concentrations of CHP and Cu^{2+} in (c-f) are 100 and 300 µM. The error bars in (a) to (d) represent standard errors of the mean (3 -5 samples per data point, a, b). The error bars for x- and y-axis in (e) and (f) represent experimental uncertainties of the solution concentration and signal integration of EPR spectra, respectively.
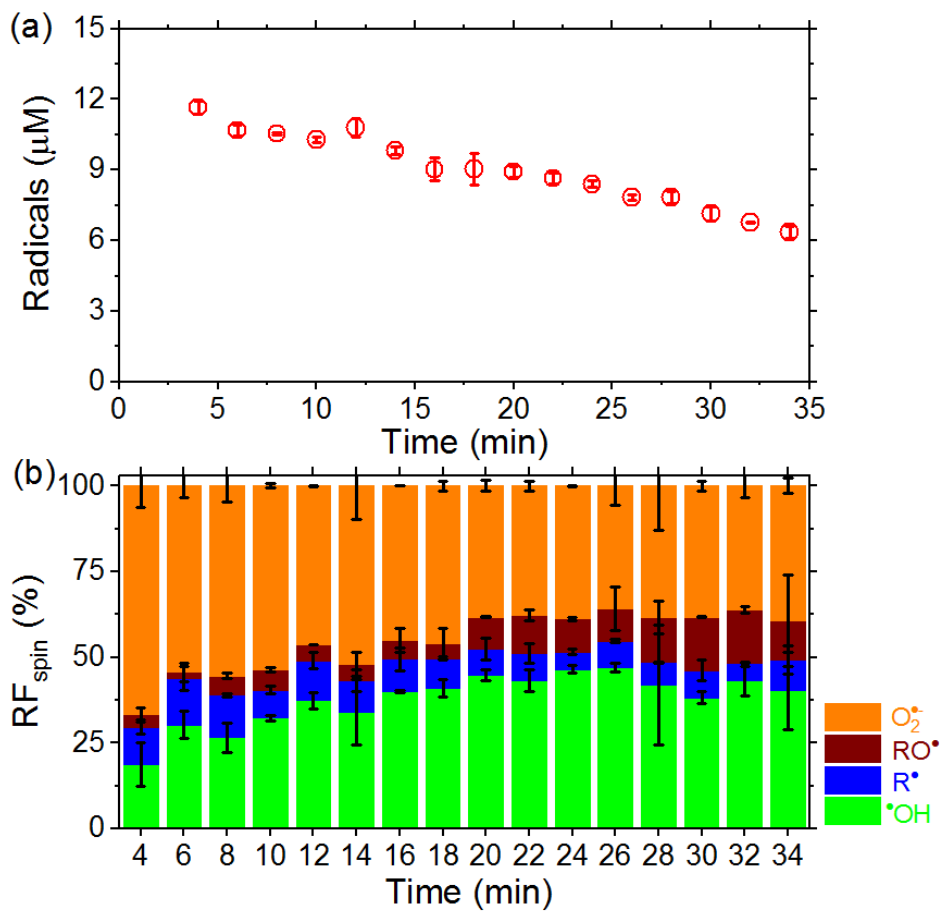
Figure S7. (a) Temporal evolution of total radical concentration and (b) relative fractions (RF) of individual radical species in aqueous mixtures of 100 µM CHP and 300 µM Fe^{2+}. Error bars represent standard deviation of duplicate measurements.

References

Aeschbacher, M., Graf, C., Schwarzenbach, R. P., and Sander, M.: Antioxidant properties of humic substances, Environ. Sci. Technol., 46, 4916-4925, 2012.

Arellanes, C., Paulson, S. E., Fine, P. M., and Sioutas, C.: Exceeding of Henry's law by hydrogen peroxide associated with urban aerosols, Environ. Sci. Technol., 40, 4859-4866, 2006.

Badali, K., Zhou, S., Aljawhary, D., Antiñolo, M., Chen, W., Lok, A., Mungall, E., Wong, J., Zhao, R., and Abbatt, J.: Formation of hydroxyl radicals from photolysis of secondary organic aerosol material, Atmos. Chem. Phys., 15, 7831-7840, 2015.

Baduel, C., Voisin, D., and Jaffrezo, J.-L.: Comparison of analytical methods for Humic Like Substances (HULIS) measurements in atmospheric particles, Atmos. Chem. Phys., 9, 5949-5962, 2009.

Chan, A. W. H., Kautzman, K., Chhabra, P., Surratt, J., Chan, M., Crounse, J., Kürten, A., Wennberg, P., Flagan, R., and Seinfeld, J.: Secondary organic aerosol formation from photooxidation of naphthalene and alkylnaphthalenes: implications for oxidation of intermediate volatility organic compounds (IVOCs), Atmos. Chem. Phys., 9, 3049-3060, 2009.

Chen, Q., Liu, Y., Donahue, N. M., Shilling, J. E., and Martin, S. T.: Particle-phase chemistry of secondary organic material: modeled compared to measured O: C and H: C elemental ratios provide constraints, Environ. Sci. Technol., 45, 4763-4770, 2011.

Chevallier, E., Jolibois, R. D., Meunier, N., Carlier, P., and Monod, A.: "Fenton-like" reactions of methylhydroperoxide and ethylhydroperoxide with Fe^{2+} in liquid aerosols under tropospheric conditions, Atmos. Environ., 38, 921-933, 2004.

Docherty, K. S., Wu, W., Lim, Y. B., and Ziemann, P. J.: Contributions of organic peroxides to secondary aerosol formed from reactions of monoterpenes with O_3, Environ. Sci. Technol., 39, 4049-4059, 2005.

Floyd, R. A., and Wiseman, B. B.: Spin-trapping free radicals in the autooxidation of 6-hydroxydopamine, Biochim. Biophys. Acta, 586, 196-207, 1979.

Hakola, H., Hellén, H., Hemmilä, M., Rinne, J., and Kulmala, M.: In situ measurements of volatile organic compounds in a boreal forest, Atmos. Chem. Phys., 12, 11665-11678, 2012.

Han, J., Wang, S., Yeung, K., Yang, D., Gu, W., Ma, Z., Sun, J., Wang, X., Chow, C.-W., and Chan, A. W.: Proteome-wide effects of naphthalene-derived secondary organic aerosol in BEAS-2B cells are caused by short-lived unsaturated carbonyls, Proc. Natl. Acad. Sci. U.S.A., 10.1073/pnas.2001378117, 2020.

Huang, G., Liu, Y., Shao, M., Li, Y., Chen, Q., Zheng, Y., Wu, Z., Liu, Y., Wu, Y., Hu, M., Li, X., Lu, S., Wang, C., Liu, J., Zheng, M., and Zhu, T.: Potentially Important Contribution of Gas-Phase Oxidation of Naphthalene and Methylnaphthalene to Secondary Organic Aerosol during Haze Events in Beijing, Environ. Sci. Technol., 53, 1235-1244, 2019.

Huang, W., Zhang, Y., Zhang, Y., Zeng, L., Dong, H., Huo, P., Fang, D., and Schauer, J. J.: Development of an automated sampling-analysis system for simultaneous measurement of reactive oxygen species (ROS) in gas and particle phases: GAC-ROS, Atmos. Environ., 134, 18-26, 2016.

Huang, W., Fang, D., Shang, J., Li, Z., Zhang, Y., Huo, P., Liu, Z., Schauer, J. J., and Zhang, Y.: Relative impact of short-term emissions controls on gas and particle-phase oxidative potential during the 2015 China Victory Day Parade in Beijing, China, Atmos. Environ., 183, 49-56, 2018.

Hung, H.-F., and Wang, C.-S.: Experimental determination of reactive oxygen species in Taipei aerosols, J. Aerosol Sci., 32, 1201-1211, 2001.

Jimenez, J. L., Canagaratna, M., Donahue, N., Prevot, A., Zhang, Q., Kroll, J. H., DeCarlo, P. F., Allan, J. D., Coe, H., and Ng, N.: Evolution of organic aerosols in the atmosphere, Science, 326, 1525-1529, 2009.

Kalyanaraman, B., Darley-Usmar, V., Davies, K. J., Dennery, P. A., Forman, H. J., Grisham, M. B., Mann, G. E., Moore, K., Roberts II, L. J., and Ischiropoulos, H.: Measuring reactive oxygen and nitrogen species with fluorescent probes: challenges and limitations, Free Radic. Biol. Med., 52, 1-6, 2012.

Katsumi, N., Miyake, S., Okochi, H., Minami, Y., Kobayashi, H., Kato, S., Wada, R., Takeuchi, M., Toda, K., and Miura, K.: Humic-like substances global levels and extraction methods in aerosols, Environ. Res. Lett., 17, 1023-1029, 2019.

Kautzman, K., Surratt, J., Chan, M., Chan, A., Hersey, S., Chhabra, P., Dalleska, N., Wennberg, P., Flagan, R., and Seinfeld, J.: Chemical composition of gas-and aerosol-phase products from the photooxidation of naphthalene, J. Phys. Chem. A, 114, 913-934, 2010.

King, L., and Weber, R.: Development and testing of an online method to measure ambient fine particulate reactive oxygen species (ROS) based on the 2',7'-dichlorofluorescin (DCFH) assay, Atmos. Meas. Tech., 6, 1647-1658, 2013.

Kogut, M. B., and Voelker, B. M.: Strong copper-binding behavior of terrestrial humic substances in seawater, Environ. Sci. Technol., 35, 1149-1156, 2001.

Kourtchev, I., Ruuskanen, T., Keronen, P., Sogacheva, L., Dal Maso, M., Reissell, A., Chi, X., Vermeylen, R., Kulmala, M., Maenhaut, W., and Claeys, M.: Determination of isoprene and α‐/β‐pinene oxidation products in boreal forest aerosols from Hyytiälä, Finland: diel variations and possible link with particle formation events, Plant Biol., 10, 138-149, 2008.

Kuang, B. Y., Lin, P., Huang, X., and Yu, J. Z.: Sources of humic-like substances in the Pearl River Delta, China: positive matrix factorization analysis of $PM_{2.5}$ major components and source markers, Atmos. Chem. Phys., 15, 1995-2008, 2015.

Lang, J., Zhang, Y., Zhou, Y., Cheng, S., Chen, D., Guo, X., Chen, S., Li, X., Xing, X., and Wang, H.: Trends of $PM_{2.5}$ and chemical composition in Beijing, 2000–2015, Aerosol Air Qual. Res., 17, 412-425, 2017.

Lazrus, A. L., Kok, G. L., Gitlin, S. N., Lind, J. A., and McLaren, S. E.: Automated fluorimetric method for hydrogen peroxide in atmospheric precipitation, Anal. Chem., 57, 917-922, 1985.

Lee, A., Goldstein, A. H., Keywood, M. D., Gao, S., Varutbangkul, V., Bahreini, R., Ng, N. L., Flagan, R. C., and Seinfeld, J. H.: Gas‑phase products and secondary aerosol yields from the ozonolysis of ten different terpenes, J. Geophys. Res., 111, D07302, 2006.

Li, X., Han, J., Hopke, P. K., Hu, J., Shu, Q., Chang, Q., and Ying, Q.: Quantifying primary and secondary humic-like substances in urban aerosol based on emission source characterization and a source-oriented air quality model, Atmos. Chem. Phys., 19, 2327-2341, 2019.

Lin, P., Engling, G., and Yu, J.: Humic-like substances in fresh emissions of rice straw burning and in ambient aerosols in the Pearl River Delta Region, China, Atmos. Chem. Phys., 10, 6487-6500, 2010.

Liu, F., Saavedra, M. G., Champion, J. A., Griendling, K. K., and Ng, N. L.: Prominent Contribution of Hydrogen Peroxide to Intracellular Reactive Oxygen Species Generated upon Exposure to Naphthalene Secondary Organic Aerosols, Environ. Sci. Technol. Lett., 7, 171-177, 2020.

Peng, Z., and Jimenez, J. L.: Radical chemistry in oxidation flow reactors for atmospheric chemistry research, Chem. Soc. Rev., 49, 2570-2616, 2020.

Perrone, M. G., Zhou, J., Malandrino, M., Sangiorgi, G., Rizzi, C., Ferrero, L., Dommen, J., and Bolzacchini, E.: PM chemical composition and oxidative potential of the soluble fraction of particles at two sites in the urban area of Milan, Northern Italy, Atmos. Environ., 128, 104-113, 2016.

Scheinhardt, S., Müller, K., Spindler, G., and Herrmann, H.: Complexation of trace metals in size-segregated aerosol particles at nine sites in Germany, Atmos. Environ., 74, 102-109, 2013.

See, S., Wang, Y., and Balasubramanian, R.: Contrasting reactive oxygen species and transition metal concentrations in combustion aerosols, Environ. Res., 103, 317-324, 2007.

Tan, J., Xiang, P., Zhou, X., Duan, J., Ma, Y., He, K., Cheng, Y., Yu, J., and Querol, X.: Chemical characterization of humic-like substances (HULIS) in $PM_{2.5}$ in Lanzhou, China, Sci. Total Environ., 573, 1481-1490, 2016.

Tong, H., Arangio, A. M., Lakey, P. S., Berkemeier, T., Liu, F., Kampf, C. J., Brune, W. H., Pöschl, U., and Shiraiwa, M.: Hydroxyl radicals from secondary organic aerosol decomposition in water, Atmos. Chem. Phys., 16, 1761-1771, 2016.

Tong, H., Lakey, P. S., Arangio, A. M., Socorro, J., Kampf, C. J., Berkemeier, T., Brune, W. H., Pöschl, U., and Shiraiwa, M.: Reactive oxygen species formed in aqueous mixtures of secondary organic aerosols and mineral dust influencing cloud chemistry and public health in the Anthropocene, Faraday Discuss., 200, 251-270, 2017.

Tong, H., Lakey, P. S., Arangio, A. M., Socorro, J., Shen, F., Lucas, K., Brune, W. H., Pöschl, U., and Shiraiwa, M.: Reactive oxygen species formed by secondary organic aerosols in water and surrogate lung fluid, Environ. Sci. Technol., 52, 11642-11651, 2018.

Tong, H., Zhang, Y., Filippi, A., Wang, T., Li, C., Liu, F., Leppla, D., Kourtchev, I., Wang, K., Keskinen, H.-M., Levula, J. T., Arangio, A. M., Shen, F., Ditas, F., Martin, S. T., Artaxo, P., Godoi, R. H. M., Yamamoto, C. I., Souza, R. A. F. d., Huang, R.-J., Berkemeier, T., Wang, Y., Su, H., Cheng, Y., Pope, F. D., Fu, P., Yao, M., Pöhlker, C., Petäjä, T., Kulmala, M., Andreae, M. O., Shiraiwa, M., Pöschl, U., Hoffmann, T., and Kalberer, M.: Radical Formation by Fine Particulate Matter Associated with Highly Oxygenated Molecules, Environ. Sci. Technol., 53, 12506-12518, 2019.

Venkatachari, P., Hopke, P. K., Grover, B. D., and Eatough, D. J.: Measurement of particle-bound reactive oxygen species in Rubidoux aerosols, J. Atmos. Chem., 50, 49-58, 2005.

Verma, V., Wang, Y., El-Afifi, R., Fang, T., Rowland, J., Russell, A. G., and Weber, R. J.: Fractionating ambient humic-like substances (HULIS) for their reactive oxygen species activity–Assessing the importance of quinones and atmospheric aging, Atmos. Environ., 120, 351-359, 2015.

Wang, H., and Joseph, J. A.: Quantifying cellular oxidative stress by dichlorofluorescein assay using microplate reader, Free Radic. Biol. Med., 27, 612-616, 1999.

Wang, Y., Arellanes, C., Curtis, D. B., and Paulson, S. E.: Probing the source of hydrogen peroxide associated with coarse mode aerosol particles in Southern California, Environ. Sci. Technol., 44, 4070-4075, 2010.

Wang, Y., Hopke, P. K., Sun, L., Chalupa, D. C., and Utell, M. J.: Laboratory and field testing of an automated atmospheric particle-bound reactive oxygen species sampling-analysis system, J. Toxicol., 2011, 419476, 2011.

Wang, Y., Arellanes, C., and Paulson, S. E.: Hydrogen peroxide associated with ambient fine-mode, diesel, and biodiesel aerosol particles in Southern California, Aerosol Sci. Technol., 46, 394-402, 2012.

Wragg, F., Fuller, S. J., Freshwater, R., Green, D. C., Kelly, F. J., and Kalberer, M.: An automated online instrument to quantify aerosol-bound reactive oxygen species (ROS) for ambient measurement and health-relevant aerosol studies, Atmos. Meas. Tech., 9, 4891-4900, 2016.

Zhang, X., McVay, R. C., Huang, D. D., Dalleska, N. F., Aumont, B., Flagan, R. C., and Seinfeld, J. H.: Formation and evolution of molecular products in α-pinene secondary organic aerosol, Proc. Natl. Acad. Sci. U.S.A., 112, 14168-14173, 2015.

Zhou, J., Bruns, E. A., Zotter, P., Stefenelli, G., Prévôt, A. S., Baltensperger, U., El-Haddad, I., and Dommen, J.: Development, characterization and first deployment of an improved online reactive oxygen species analyzer, Atmos. Meas. Tech., 11, 65-80, 2018.